Supplementary Information

Uncover the Unusual Anodic Current during Tetrafluoroborate Anion Deintercalation from Graphite Cathode in Ethylene Carbonate

Haibo Liu[a,b], Yunju Wang[c], Guobao Xu[a,b],*, Hongyu Wang[c],*

a State Key Laboratory of Electroanalytical Chemistry, Changchun Institute of Applied Chemistry, Chinese Academy of Sciences, 5625 Renmin Street, Changchun 130022, China

b School of Applied Chemistry and Engineering, University of Science and Technology of China, Hefei 230026, China

c Key Laboratory of UV Light Emitting Materials and Technology, Ministry of Education, Northeast Normal University, 5628 Renmin Street, Changchun 130024, China

* Corresponding authors.

E-mail addresses: Guobao Xu (guobaoxu@ciac.ac.cn); Hongyu Wang (hongyuwang@aliyun.com)

Content

1. Calculation of Stage Number (SN) and Intercalated Gallery Height (IGH).

According to the Bragg's law, we have

$$d_{00n+1} = \frac{\lambda}{2sin\theta_{00n+1}} = \frac{I_C}{n+1} \tag{1}$$

$$d_{00n+2} = \frac{\lambda}{2sin\theta_{00n+2}} = \frac{I_C}{n+2} \tag{2}$$

where Ic is the periodic distance and λ is the known X-ray wavelength.

Combining equations (1) with (2), the stage number n can be calculated as follow:

$$n = \frac{1}{\frac{sin\theta_{00n+2}}{sin\theta_{00n+1}} - 1} - 1 \tag{3}$$

After assigning the (00n+1) indices, the intercalation gallery height (IGH) can be calculated with following equation:

$$I_C = IGH + (n-1) \times 0.335 \ nm \tag{4}$$

2. Sauerbrey Equation.

$$\Delta f_n = -2.26 \times 10^{-6} f^2 \Delta m / A \tag{5}$$

Among them, Δf_n is the change in the nth harmonic resonance frequency of a crystal with a fundamental frequency of f_1, Δm is the change in mass (g), and **A** is the film area (cm^2)

3. Experimental Section

3.1. **Materials and Electrode Preparation.** Natural graphite flakes supplied by BTR New Energy Materials INC were employed as the positive electrode material. Activated carbon (AC, YP-50F, Kuraray Co., Ltd.) was used as both the counter

electrode and reference electrode material. Teflonized acetylene black (TAB, Denka Co., Ltd.) acted as the conductive binder. The aluminum mesh (Hebei Anhengsiwang Co., Ltd.) served as the current collector for all the electrodes in the test cells ($\varnothing15.6$ mm for CR2032 coin cell and $\varnothing13.0$ mm for the Swagelok cells).

The active electrode material (graphite or AC) and TAB were homogeneously blended with a mass ratio of 2:1 (active material/TAB, 10.0 mg/5.0 mg in CR2032 cells, 5.0 mg/2.5 mg in Swagelok cells) by a mortar and pestle and then pressed on a piece of aluminum mesh to fabricate an electrode. Glass fiber filter (thickness, 0.44 mm, GA-100, Advantec Toyo Kaisha Ltd.) was employed as the separator. All electrodes and separators were dried at 180 °C under vacuum for 4 h to remove trace water. The series of mixed salt electrolyte solutions were prepared by dissolving the electrolyte salt of $TEABF_4$ (purity >99.0%, TCI) or $TEAPF_6$ (purity >99.0%, TCI (Shanghai) Development Co. Ltd.) in the solvent of EC (purity ≥99.99%, Shandong Senjie Chemical Co., Ltd.). Lithium tetrafluoroborate (LiBF4, purity>99.0%), lithium perchlorate ($LiClO_4$, purity>99.0%) spiro-(1,1')-bipyrrolidinium tetrafluoroborate (SBPBF4, purity>98.0%), tetrabutylammonium tetrafluoroborate ($TBABF_4$, purity>99.0%) and triethlmethylammonium tetrafluoroborate ($TEMABF_4$, purity >99.0%) were purchased from TCI (Shanghai) Development Co. Ltd. The series of $BMIMBF_4$-EC electrolyte solutions were fabricated by blending EC and the ionic liquid of $BMIMBF_4$ (purity >99%, TCI (Shanghai) Development Co. Ltd.) with varying molar ratios. EC was dried over molecular sieves at least one week before preparing the electrolyte solutions. All preparation processes are completed in a glove

box filled with argon atmosphere.

3.2. **Correlative Measurements.** Electrochemical measurements were conducted with coin cells (CR2032, Dongguan, China, Canrd New Energy Technology Co., Ltd.), beaker cells and Swagelok cells. The mass ratio of the working electrode (graphite) and counter electrode (AC) was kept at 1. The quasi-reference electrode (QRE) was activated carbon with the extra mass as compared with graphite, whose reliability has been proved previously. Cyclic voltammetric (CV) investigations were conducted in Swagelok cells in a three-electrode configuration from 0 to 2.0 V (vs. AC-QRE) with a scanning rate of 1 mV s^{-1} by an electrochemical workstation (CHI660E, Shanghai, China, Chenhua Co., Ltd.). All CV current intensity was normalized to 1 for comparison. Galvano-static tests were performed from 0 to 3.5 V at a current density of 0.1 A g^{-1} on coin cells by a battery testing system (CT4008, Shenzhen, China, Neware Co., Ltd.). The ionic conductivity of electrolyte solutions at 30 °C was tested by the conductivity meter (DDS–11A, Shanghai, REX Instrument Co., Ltd.) in a glovebox filled with pure argon atmosphere. Electrochemical impedance spectroscopic (EIS) measurements were performed on symmetric cells with two identical graphite electrodes recovered from AC/graphite cells charged to 3.5 V by an electrochemical workstation CHI660C. The frequency range was from 100 kHz to 0.01 Hz and the amplitude was 5 mV. And the EIS data was fitted by Zview software and the equivalent circuit model could be acquired. The EQCM measurement was carried out by Research Quartz Crystal Microbalance Monitor (RQCM, MAXTEK, INFICON) and Quartz crystal chips with a fundamental

frequency of approximately 5 MHz in conjunction with an electrochemical workstation CHI700D. The configuration was shown in **Figure S6**. The working electrode of quartz crystal plate was dispensed by the aqueous slurry of 90% graphite powder and 10% CMC (by weight) and then dried at 60 °C for over 4 h to drive out the water before use. The ECD measurement was performed on a two-electrode (AC/graphite) cell between 0 and 3.5 V by ECD-3-nano electrochemical dilatometer (EL-CELL, Germany). The real-time galvano-static charge-discharge was controlled by a battery testing system (LAND, CT2001A). The working electrode was graphite coating on aluminum foil (graphite/ PVDF/super-P = 8:1:1 by weight). The counter electrode was AC and the current density was 0.1 A g^{-1}.

The *ex situ* XRD characterization was implemented on graphite electrodes recovered from the AC/graphite cells charged to 3.5 V by a Rigaku MiniFlex600 X-ray diffractometer with the 2θ range between 10 and 50° under a scanning rate of 10 ° min^{-1}. In the *in situ* XRD measurements, the battery testing system CT2001T from Wuhan LAND Co., Ltd. was applied to control the charge/discharge states of the Li/graphite cells.

The NMR spectra of the electrolyte solutions were measured by Bruker ADVANCE III HD 500 using dimethyl sulfoxide-d6 (DMSO-d6) as the internal standard reagents. Experiments were carried out at the room temperature near 25 °C. Fourier transform infrared spectroscopy (FT-IR) spectra were acquired on a Bruker Vertex 70 spectrometer with region of 400-4000 cm^{-1}. A Xplora confocal microscope Raman system (Witec, Germany) was used to collect the Raman spectra.

4. Supporting figures and tables

Table S1. AGICs Parameters calculated based on *ex situ* XRD patterns of **Figure 2**.

Electrolyte Solution	Basal repeat length along C / nm	SN	IGH / nm
BMIMBF$_4$	-	-	-
EC : BMIMBF$_4$ = 0.29	-	-	-
EC : BMIMBF$_4$ = 0.57	-	-	-
EC : BMIMBF$_4$ = 1.13	2.605	6.33	0.819
EC : BMIMBF$_4$ = 2.27	2.566	6.24	0.810
EC : BMIMBF$_4$ = 5.13	2.177	5.06	0.817
EC : BMIMBF$_4$ = 9.13	2.172	5.04	0.819

\- There are no obvious peaks for calculation.
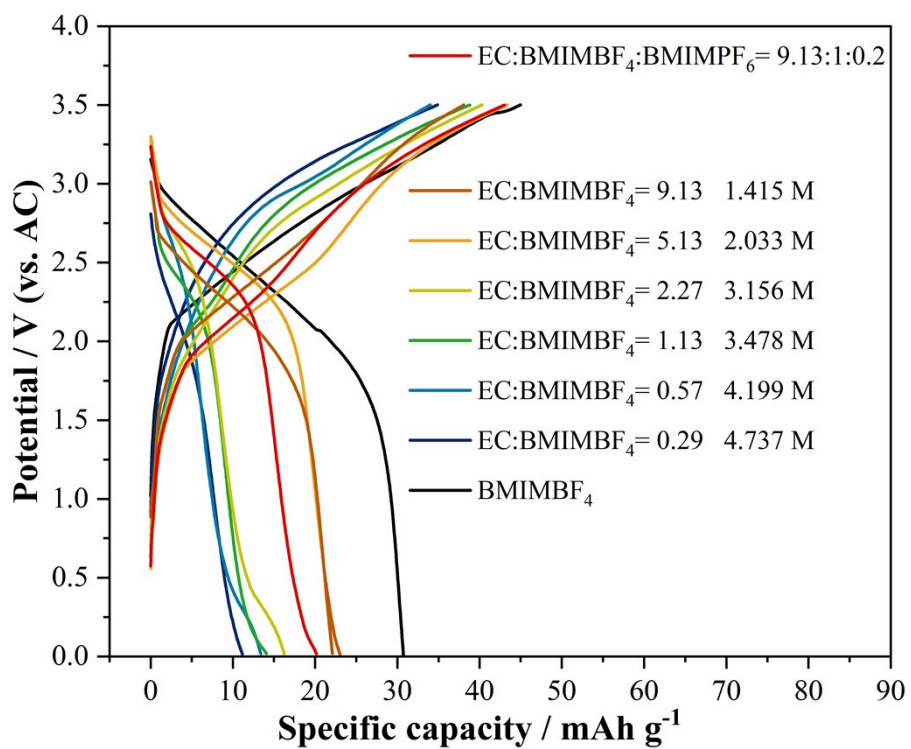
Figure S1. The initial galvanostatic charge/discharge curves of DIBs with EC-BMIMBF$_4$ and EC-BMIMBF$_4$+BMIMPF$_6$ electrolyte solutions.
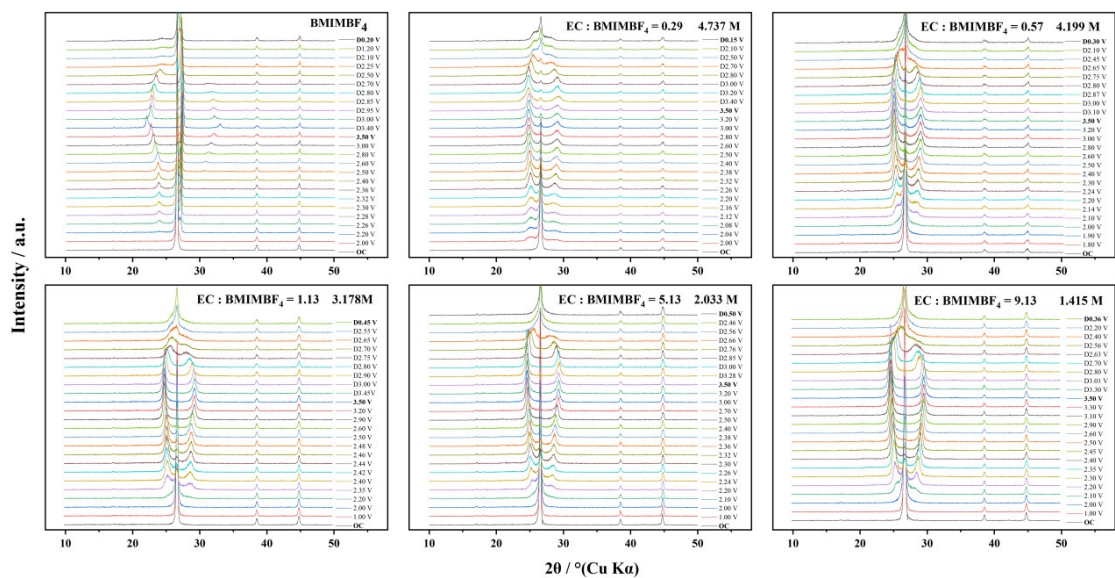
Figure S2. *In situ* XRD patterns of graphite electrodes in AC/graphite cells utilizing the electrolyte solutions of BMIMBF$_4$-EC during the initial charge–discharge cycle.
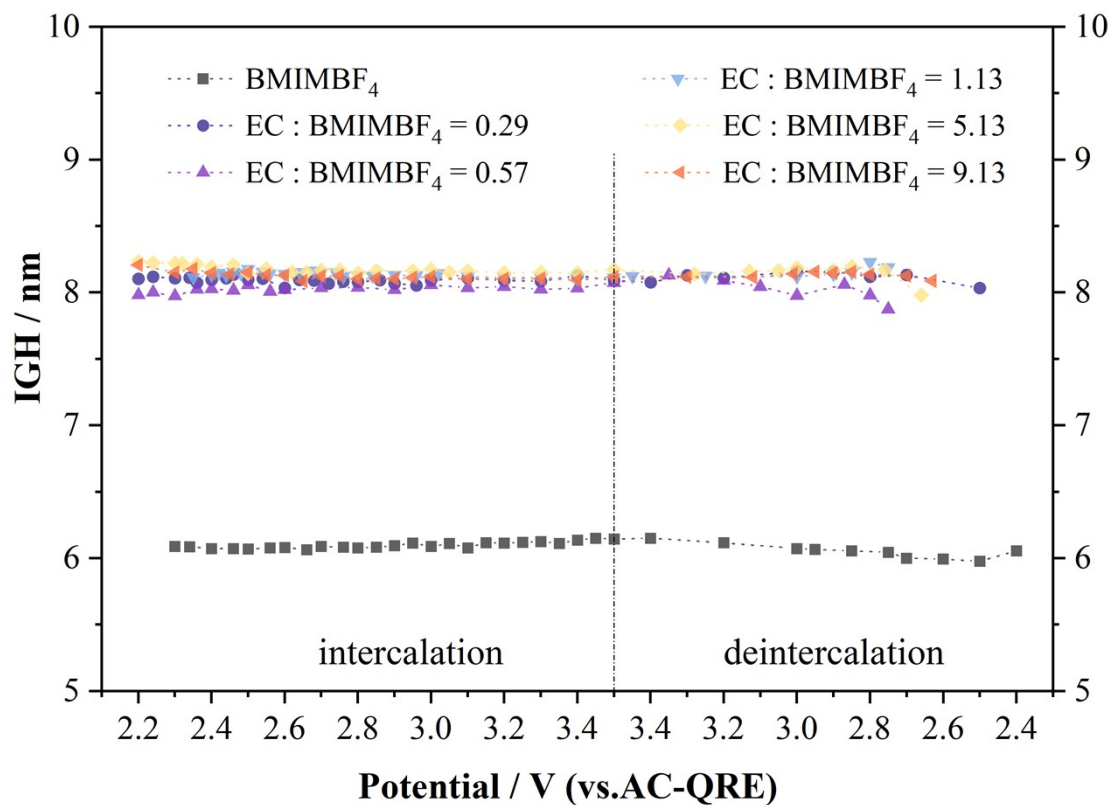
Figure S3. IGH values of AGICs utilizing the electrolyte solutions of BMIMBF$_4$-EC
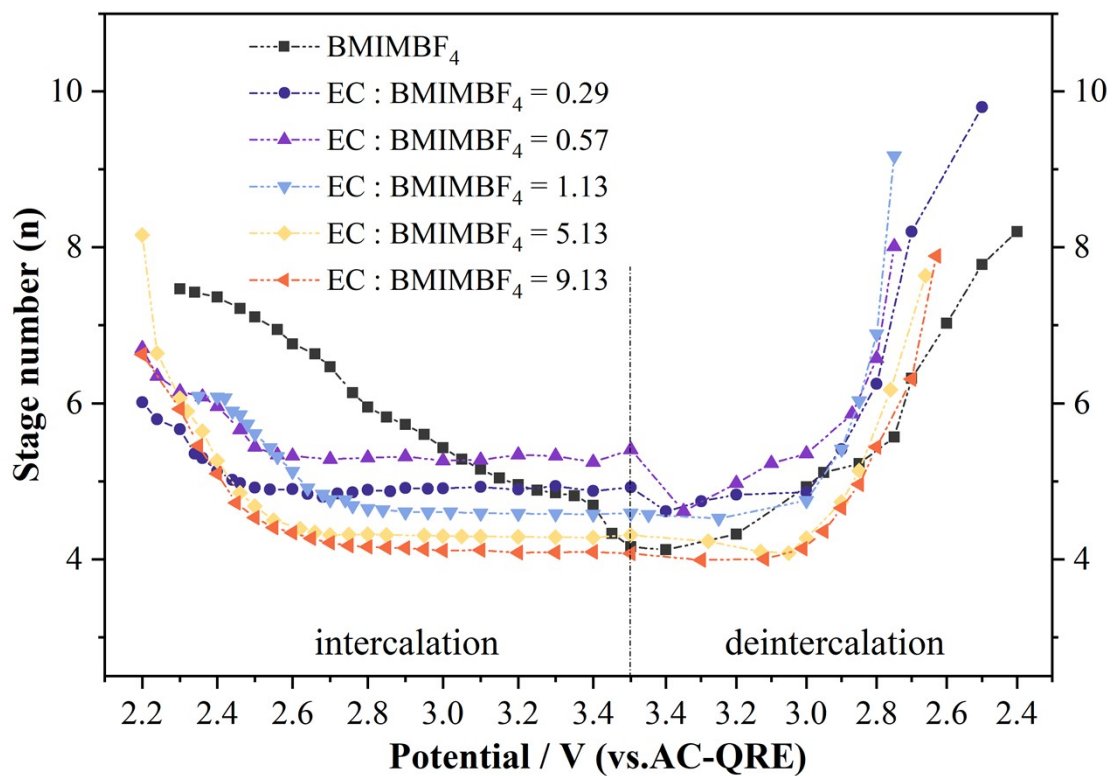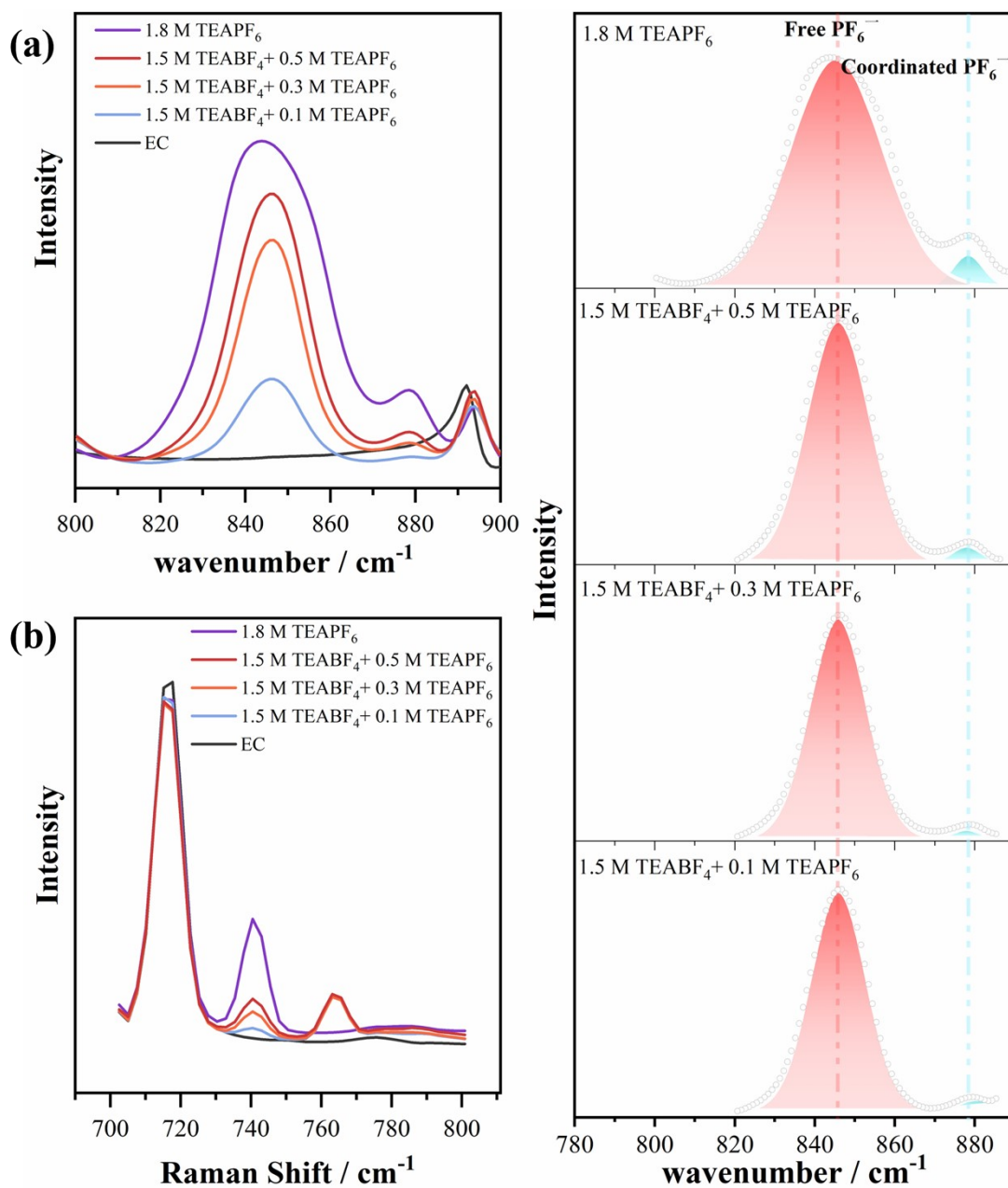
during the initial charge–discharge cycle.

Figure S4. The stage number of AGICs utilizing the electrolyte solutions of

BMIMBF$_4$-EC during the initial charge–discharge cycle.

Figure S5. (a) FT-IR spectra and (b) Raman spectra of *P-F* bond in
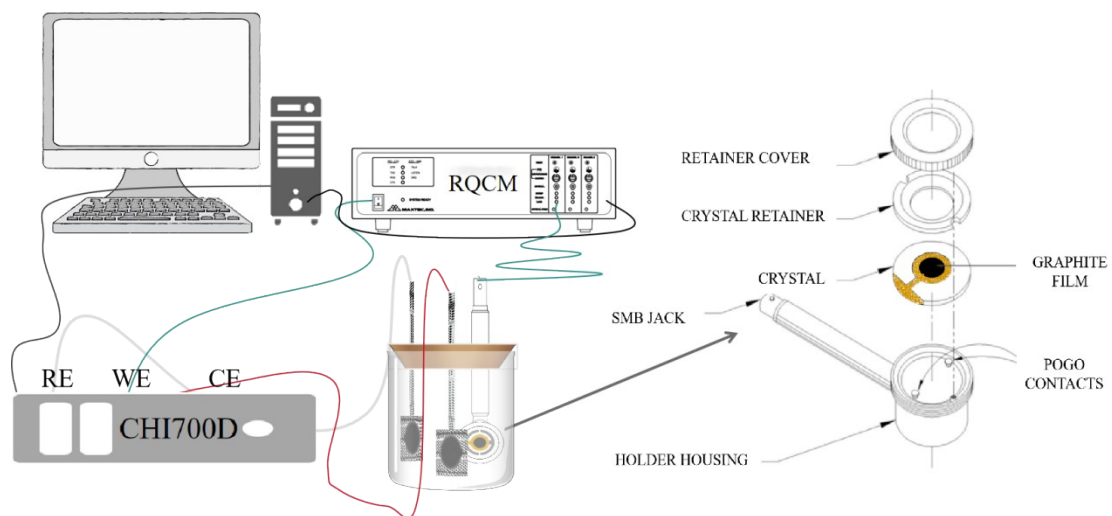
TEABF$_4$+TEAPF$_6$-EC electrolyte solutions.
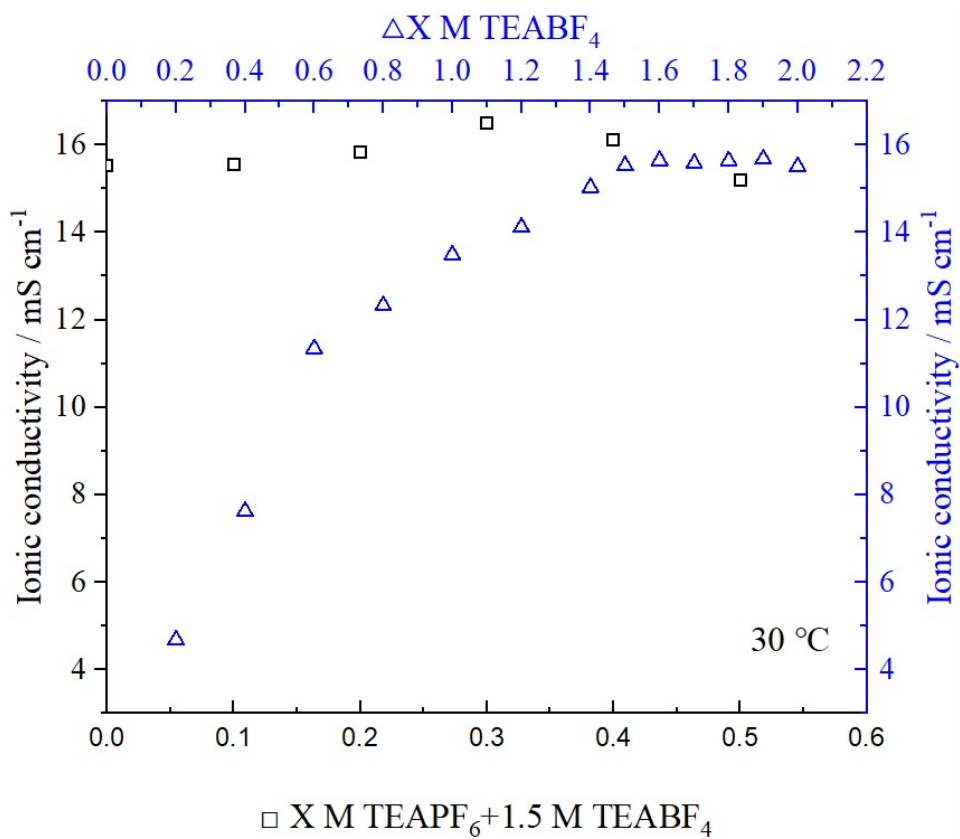
Figure S6. EQCM testing schematic diagram.

Figure S7. The ionic conductivity of TEABF$_4$-EC and TEAPF$_6$ + TEABF$_4$-EC
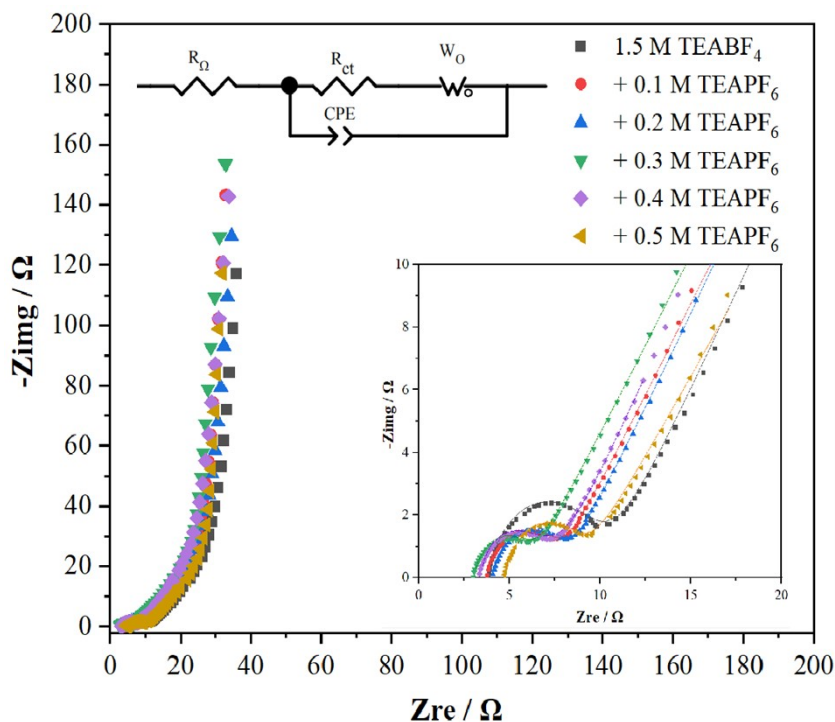
electrolyte solutions at 30 °C.

Figure S8. Nyquist plots of the graphite symmetric cells with electrolyte solutions of

$TEAPF_6 + TEABF_4$-EC.

Table S2. Element Values in the $R_\Omega(CPE(R_{ct}W_O))$ Equivalent Circuit of Impedance

Spectra of **Figure S8**.

| Electrolyte solution	R_Ω /Ω	R_{ct} /Ω	CPE-T/F	CPE-P/F	W-R /Ω · cm²	W-T /Ω · cm²	W-P /Ω · cm²
1.5 M TEABF₄	3.878	4.477	2.58E-05	0.88311	6.573	1.55E-02	0.28741
1.5 M TEABF₄ +0.1 M TEAPF₆	3.769	3.923	6.79E-05	0.80669	56.81	0.61921	0.54635
1.5 M TEABF₄ +0.2 M TEAPF₆	3.554	4.095	6.84E-05	0.80604	59.64	0.67814	0.55718
1.5 M TEABF₄ +0.3 M TEAPF₆	3.048	3.147	6.46E-05	0.83325	60.15	0.62594	0.54018
1.5 M TEABF₄ +0.4 M TEAPF₆	3.425	2.192	1.70E-05	0.93094	6.429	0.014094	0.29095
1.5 M TEABF₄ +0.5 M TEAPF₆	4.712	3.787	5.49E-05	0.82683	51.88	0.76574	0.51069
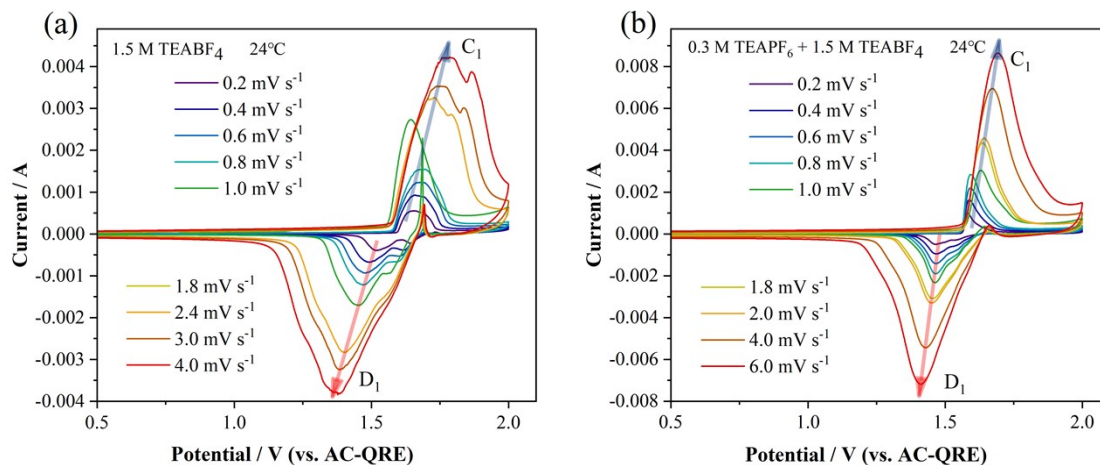
Figure S9. Cyclic voltammograms of graphite cathode in (a) 1.5 M TEABF$_4$ + 0.3 M TEAPF$_6$-EC and (b) 1.8 M TEABF$_4$-EC solutions at different scan rates.
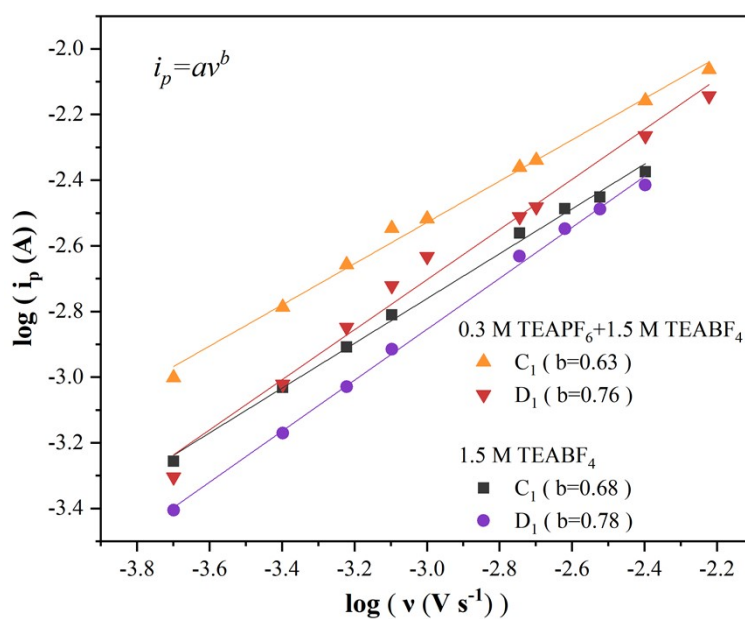

Figure S10. log (i) vs. log (v) plots according to **Figure S9.**
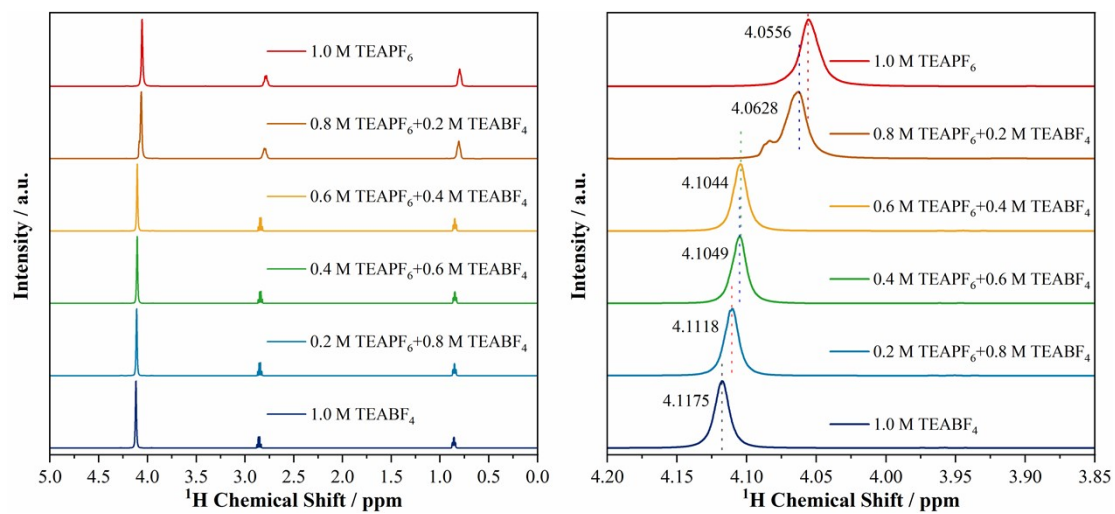
Figure S11. ^{1}H NMR spectra for the 1 M TEABF$_4$ + TEAPF$_6$-EC solutions.
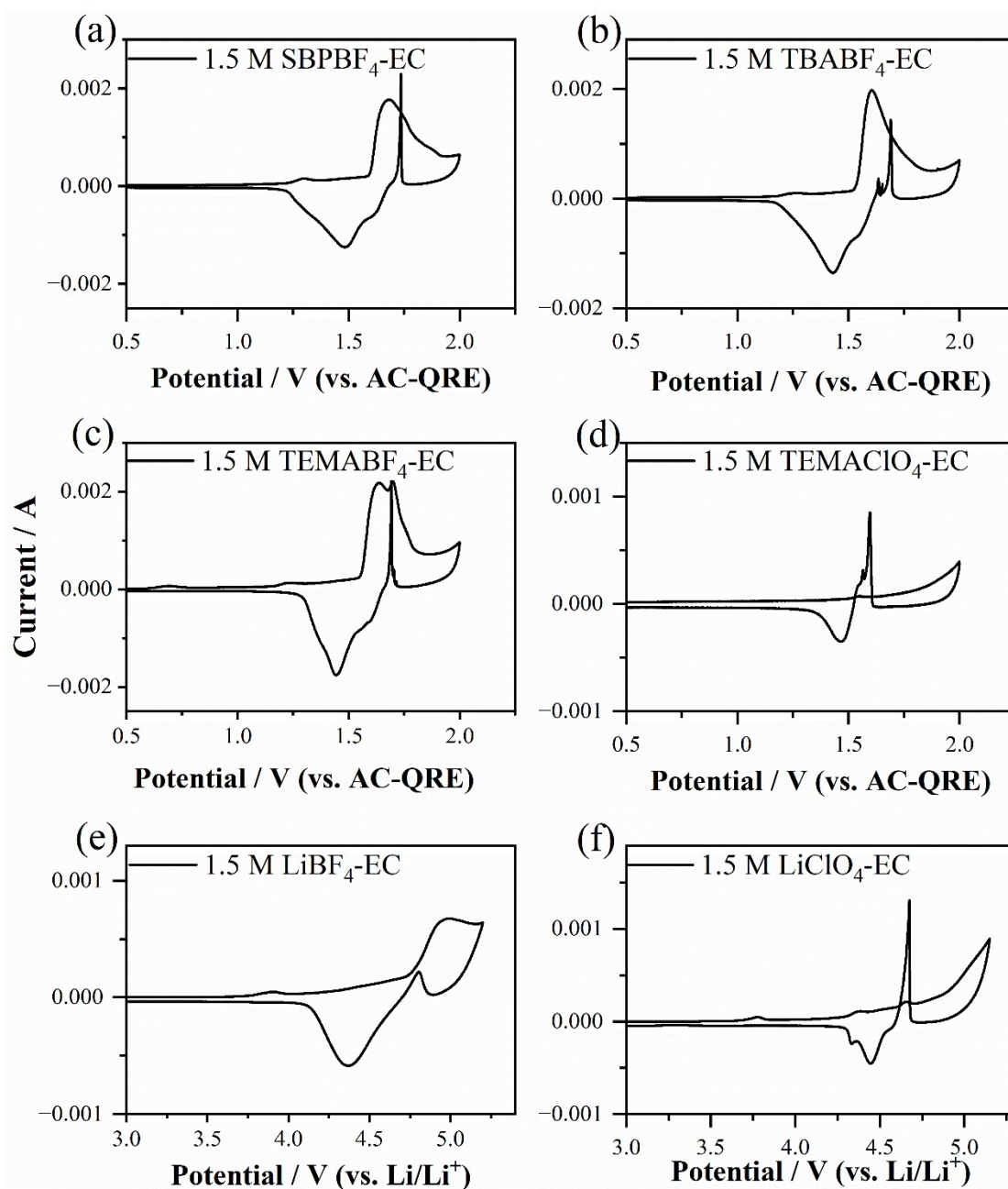
Figure S12. The counter current phenomenon in another combination of anions and

solvents. (a) SBPBF$_4$-EC (b) TBABF$_4$-EC (c) TEMABF$_4$-EC (d) TEMAClO$_4$-EC (e)

LiBF$_4$-EC (f) LiClO$_4$-EC